



HAL
open science

An experimental device for the simultaneous estimation of the thermal conductivity 3-D tensor and the specific heat of orthotropic composite materials

Matthieu Thomas, Nicolas Boyard, Nicolas Lefevre, Yvon Jarny, Didier Delaunay

► To cite this version:

Matthieu Thomas, Nicolas Boyard, Nicolas Lefevre, Yvon Jarny, Didier Delaunay. An experimental device for the simultaneous estimation of the thermal conductivity 3-D tensor and the specific heat of orthotropic composite materials. *International Journal of Heat and Mass Transfer*, 2010, 53 (23-24), pp.5487-5498. 10.1016/j.ijheatmasstransfer.2010.07.008 . hal-03960221

HAL Id: hal-03960221

<https://hal.science/hal-03960221v1>

Submitted on 27 Jan 2023

HAL is a multi-disciplinary open access archive for the deposit and dissemination of scientific research documents, whether they are published or not. The documents may come from teaching and research institutions in France or abroad, or from public or private research centers.

L'archive ouverte pluridisciplinaire **HAL**, est destinée au dépôt et à la diffusion de documents scientifiques de niveau recherche, publiés ou non, émanant des établissements d'enseignement et de recherche français ou étrangers, des laboratoires publics ou privés.

An Experimental Device for the Simultaneous Estimation of the Thermal Conductivity 3-D Tensor and the Specific Heat of Orthotropic Composite Materials

M. Thomas ^b, N. Boyard ^{a,*}, N. Lefèvre ^a, Y. Jarny ^a and D. Delaunay ^a

^a *Université de Nantes, Nantes Atlantique Universités, CNRS, Laboratoire de Thermocinétique de Nantes, UMR 6607, La Chantrerie, rue Christian Pauc, BP 50609, 44306 Nantes cedex 3 – France*

^b *Airbus, 316 Route de Bayonne, 31060 Toulouse - France*

*Corresponding author nicolas.boyard@univ-nantes.fr

Phone: +33 2 40 68 31 15, Fax: +33 2 40 68 31 41

Abstract:

In this study, a new experimental design, which has the advantage of estimating simultaneously the three components of the thermal conductivity tensor and the specific heat of orthotropic polymer composite materials is presented. Furthermore, no sample instrumentation is required, reducing substantially the global experimental procedure duration. The measurement technique consists in dissipating a known heat flux thanks to a home-designed thin heater, composed by two distinct heating elements and sandwiched between two cylindrical samples. The heater is also used as measurement instrument since micro thermocouples are incorporated inside. The parameter estimation is performed by an inverse method. The method has been validated on a sample with known properties. The thermal properties of a unidirectional carbon-fiber composite have been then characterized. The results, obtained from a two-step estimation strategy are in good agreement with those determined within the framework of round-robin test.

Nomenclature

C_p	specific heat [J/kg.K]	ϕ	heat flux [W/m ²]
C	correlation matrix	Γ	face of domain
e	thickness [m]	λ	thermal conductivity
n	normal vector		[W/m.K]
t	time [s]	Λ	thermal conductivity tensor
t_0	initial time [s]	θ	rotation angle between
r	radius of heater element [m]		coordinates
re	relative error	ρ	density [kg/m ³]
R_{tc}	thermal contact resistance [m ² K/W]	σ	Stephan constant
T	temperature [K]	σ_N	standard deviation
T_∞	initial temperature [K]	Ω	spatial domain
X	sensitivity		
X^*	reduced sensitivity [K]		
			<i>Main subscripts</i>
		int	interior
		ext	exterior
		Oxyz	sample coordinates
		OXYz	heater coordinates
		A	heating configuration A
		B	heating configuration B
		s	sensor
	<i>Greek symbols</i>		
β	parameter vector		
χ	characteristic function		
δ_{ij}	Kronecker symbol		
ε	emissivity		

Key words: composite material, thermal properties,

1. Introduction

Composite materials are most often an innovative technological solution to improve and create more competitive products in many industrial sectors. Their properties offer numerous advantages compared to those of traditional materials (lightness, strength, chemical resistance, complex forms, noise, vibration, etc.). Moreover, cost-effective composite parts can be manufactured by utilizing proper design and manufacturing techniques. Composites offer design freedom by tailoring material properties to meet performance specifications, thus avoiding the over-design of products. All these reasons have led to a considerable development of these materials and their diversity.

In leading-edge domains such as aeronautics, the high-performances of composites are an undeniable asset. Metals are then gradually substituted by composites in airplane structures. However, even if it has great advantages for mechanical issues, it can also induce "collateral" concerns. Thermal problems are among the crucial ones. In fact, composite materials are so insulating compared to metallic materials that rapidly heat confinement problems occur. To predict the thermal environment of airplane structure, thermal properties of involved composite structures as well as the uncertainties relative to their measurements are thus required. To satisfy this need, the determination of the thermal properties of composite materials is addressed in this study. Note that the term "composite" is here restricted to polymer matrix reinforced with carbon fibres. Two parallel means can be considered for this issue:

- The development and the use of predictive heat conduction models is an approach to explore. The estimation of effective thermal properties from the composite microstructure is very attractive. First, once developed, they are cheap means of estimation. Then, their applications can become in the future very interesting for the design of composite with desired properties. However, this approach is not the aim of this article and has already been discussed in an other reference [1].

- Secondly, the experimental approach. The measurement of effective thermal properties on samples employing a dedicated device is another possibility to investigate. Many measurement devices have been developed to characterize orthotropic material. Realizing an exhaustive bibliography on all existing measurement methods (devices and estimation procedures) of thermal properties is an extremely large task. We therefore

limit it to our subject of interest, that is to say, the methods used to characterize organic matrix composite materials. Methods assuming the isotropic behaviour of the material are, by the way, excluded. Moreover, the organic matrix (thermosetting resins, thermoplastics) of the composite implies relatively low temperature of measurements (up to 150°C). The devices dedicated to high temperature measurements are thereby not addressed.

The thermal properties to characterize are essentially

- the components of the effective thermal conductivity tensor, Λ
- the specific heat, C_p

The density ρ is assumed to be known. When heat conduction models are supposed to be non-thermal dependent, other parameters can be characterized like the thermal diffusivity tensor $A = \Lambda / (\rho \times C_p)$ and/or the effusivity tensor $B = \sqrt{\Lambda \rho C_p}$.

In this paper, we consider that composite samples have a cylindrical shape. We assume that the size, especially the thickness in the range 5 to 50mm, is enough to define an effective thermal conductivity tensor. For convenience, we will adopt the orthogonal coordinate system $Oxyz$, where the cylinder axis is called the “transverse” direction (Oz), whereas (Ox) and (Oy) are in-plane directions. In a pure unidirectional composite, we suppose that (Ox) matches the fibres direction, and that (Oy) is orthogonal to the fibres direction. Then these directions are the main directions of the composite, and the thermal conductivity or diffusivity tensors are diagonal [2].

Many measurement devices and methods have been developed to characterize the components of these tensors. Basically, they consist in thermally exciting a sample (with electrical heater, heat flux pulse, laser,...) and measuring its thermal response (with thermocouples, IR camera, flux meter,...) so as to estimate its heat conduction properties. Degiovanni [3] realized a complete review of the main measurement methods. One can distinguish steady state methods (time independent), which only permit to determine thermal conductivities, from transient methods, for which the measurement of the thermal response is performed as a function of time. Using these latter methods, more thermal properties can be identified, like diffusivities, and specific heat.

The Guarded Hot Plate (G.H.P) is one of the most well-known steady state methods, which permits to measure a thermal conductivity along a unique direction. Many devices were developed so as to provide the most accurate results. In its first version, G.H.P. device consists of a symmetric assembly of two samples, two cold plates and one heater located on the mid plane, which dissipates a known heat flux. This method has the advantage of being simple, accurate and standardized (standard: ISO 8302 [4]). However, it has also some drawbacks, as the long period of steady state establishment, or the heavy devices used to limit the lateral heat losses and thus ensure the heat flux to be unidirectional. Moreover, compared to transient methods, this method does not permit to assess specific heat or diffusivities. The main drawback of this method may lie in the fact that it only permits to estimate a unique conductivity parameter λ_{zz} in the transverse direction. It is, however, possible to measure the other thermal conductivity parameters (λ_{xx} and λ_{yy}), but the sample has to be machined and re-shaped so as to make the heat flux cross along the desired direction while keeping a good ratio aspect. Such process obviously adds measurement uncertainties and is very time-consuming. Moreover, these measurements assume the composite main directions (Ox and Oy) are to be known.

The heating wire method ([5]-[7]) was adapted to the characterization of orthotropic materials. The method [8] uses an inverse method to estimate, the thermal conductivity parameters in both directions orthogonal to the wire, as well as the specific heat Cp. This method consists in a symmetrical assembly in which an electrical heating wire is sandwiched between two pairs of samples. The assembly is insulated on lateral faces, and micro-thermocouples are located in some grooves on sample surfaces. The wire is assumed to have a negligible radius. For enough short time of heating, the hypothesis of an infinite sample can be considered (the boundary effects are thus neglected). Initially, the assembly is isothermal, the temperature being imposed with thermo-controlled plates. At $t > 0$, the wire aligned along (Oy) direction is powered and dissipates a known constant power q_0 . Due to the anisotropic character of the composite samples, isothermal surfaces are elliptic in the plane (Oxz) orthogonal to the wire direction. Only the temperature rises of two thermocouples are required to identify by inverse method the parameters λ_{xx} , λ_{zz} , and ρC_p . Repeating the measurements by aligning the hot wire along Ox direction, an estimation of λ_{yy} is possible. The

repeatability of this method is about 5%. However, this method does not take into account the thermal inertia of the hot wire as well as the possible thermal contact resistance between the wire and the sample. As these parameters only have an influence on the temperature increase for short periods, they do not influence the estimation of the conductivities that are performed after a certain period. Nevertheless, the specific heat is mainly sensitive to short time. Precautions have thereby to be taken. Nonetheless, the main drawback of this method is the instrumentation, since the wire and the micro thermocouples have to be placed on the sample. This step is first of all time consuming. Moreover, it induces result uncertainties linked to the uncertainty of thermocouple locations.

Transient Plane Source methods (TPS) derived from works realized by Gustafsson [9]-[10] who developed a technique able to simultaneously estimate the thermal conductivity and diffusivity of homogeneous and isotropic solids. TPS methods consist of a flat heating element in the shape of a strip, strip pattern, disk, or disk pattern, that can be sandwiched either between two identical pieces of the sample (double-sided configuration) or applied to only one sample piece (single-sided configuration). When powered, the heat generated by Joule effect is dissipated through the sample. Then, from the measurement of the temperature increase of the probe, thermal properties can be calculated.

Different formats of sensors were developed to accommodate a large variety of samples. Recent developments were initiated so as to estimate the in-plane $\lambda_{xx} = \lambda_{yy}$ and the transverse λ_{zz} thermal properties of orthotropic materials [11]. The main advantage of these methods lies in the fact that both thermal conductivity and diffusivity are estimated. Moreover, the used probe generally constitutes both heat source and temperature sensor (thermocouples can be placed inside the probe), which is convenient for different aspects: ease of application, rapid instrumentation time or uncertainty on thermocouple locations.

Flash method is widely used to estimate the diffusivity of homogeneous and isotropic materials. It was extended to composite materials. In its first version, this method is built upon the analysis of the back face temperature rise of a sample whose front face is submitted to an energy pulse of short time compared to the observed phenomenon. Another method, derived from the traditional one, enables to assess in-

plane thermal diffusivity. This technique is based on a heterogeneous excitation upon one face of the sample so that thermal gradients are developed on the plane orthogonal to the excitation direction. Initially proposed by Donaldson *et al* [12] to estimate both radial and transverse diffusivity, many extensions [13]-[18] were developed and the whole thermal diffusivity tensor can be characterized. Measurement of the in-plane thermal gradients can be performed with thermocouples, but the uncertainty linked to their locations remains a problem. The use of IR-camera [19]-[20] prevents from this problem, but a high number of thermographic images is required to remain accurate. The Flash method uncertainty factors are mainly due to the experimental conditions [21] that are difficult to realize. The convective and radiative exchanges on front and back faces [22]-[23], the duration and non-homogeneity of the incident heat flux [24] or the non-linear effects. We have also to keep in mind that flash methods do not lead directly to the thermal conductivity tensor but to the thermal diffusivity tensor, because it is not possible to measure accurately the heat flux density entering the sample.

The periodic methods for the determination of thermal diffusivity are based on a theory originally stated by Ångström [25]. The principle consists in heating periodically a sample, then the temperature along the sample also varies with the same period, but with an amplitude that decays exponentially. Moreover, the measurement of phase lag between periodic input and thermal response of the material can be directly related to the thermal diffusivity. Many other models and experimental devices [26] are based on Ångström's method to measure heat transfer coefficients [27], thermal diffusivity of anisotropic media [28], or thermal properties on small dimension media (e.g. thermal properties of fibres contained in composite materials [29]-[30]).

We have pointed out that the measurements of the whole thermal conductivity tensor and the specific heat require to combine and/or repeat different experimental methods. This generally involves the use of multiple composite samples, or successive tooling steps of the sample to adapt it to the different measurement devices employed. Resulting uncertainty may consequently be important.

Our research has focussed on the development of a new experimental device that is able to simultaneously assess the components of thermal conductivity tensor and the specific heat of composite materials. The measurement technique consists in dissipating

a known heat flux thanks to a thin heater sandwiched between two cylindrical samples. The heater is composed by two distinct heating elements and is also used as measurement instrument since micro thermocouples are incorporated inside. The parameters estimation is performed by an inverse method.

2. General presentation of the experimental device

Experimental device (Figure 1) consists in a thin electrical heater, sandwiched between two similar composite samples. The symmetrical assembly (heater and samples) is located in a thermo-regulated vacuum chamber.

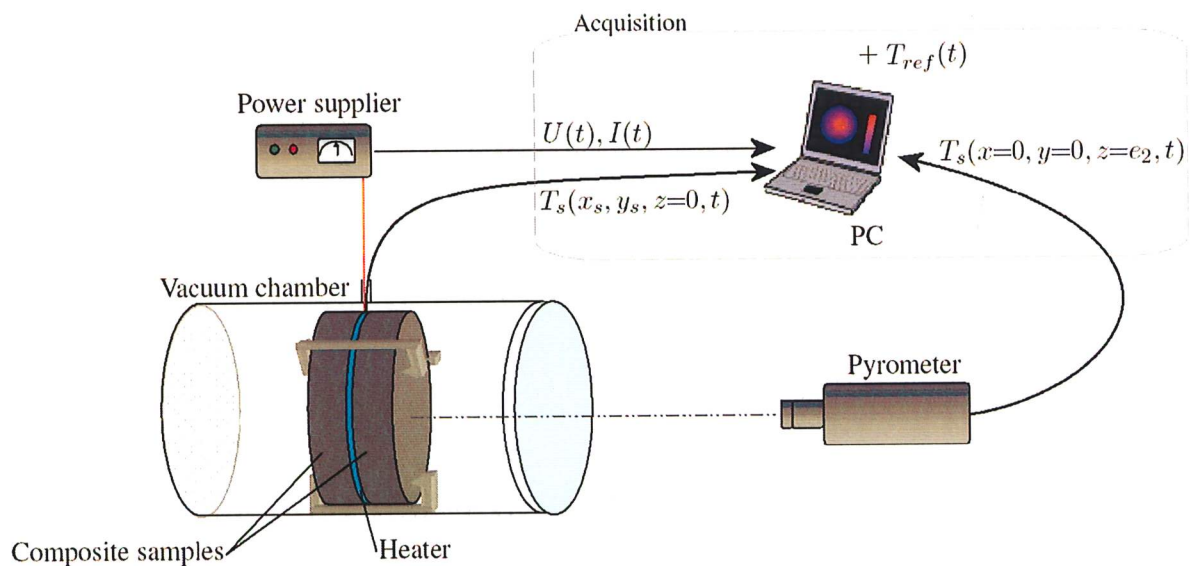


Figure 1: Schematic presentation of the experimental device.

The heater (Figure 2) serves as both heat source and temperature measurement device. Its development required several tests and experiments. The final version presented here is composed of a stack of Kapton discs on which are set two distinct circular heating tracks: a central heating disc of radius r_{int} , and a peripheral heating corona between the interior radius r_{int} and the exterior radius $r_{ext} = 60\text{mm}$. Fourteen T-type micro-thermocouples ($30\ \mu\text{m}$ thick) are located on the heater (seven per face), along three different directions, at different radii from the centre.

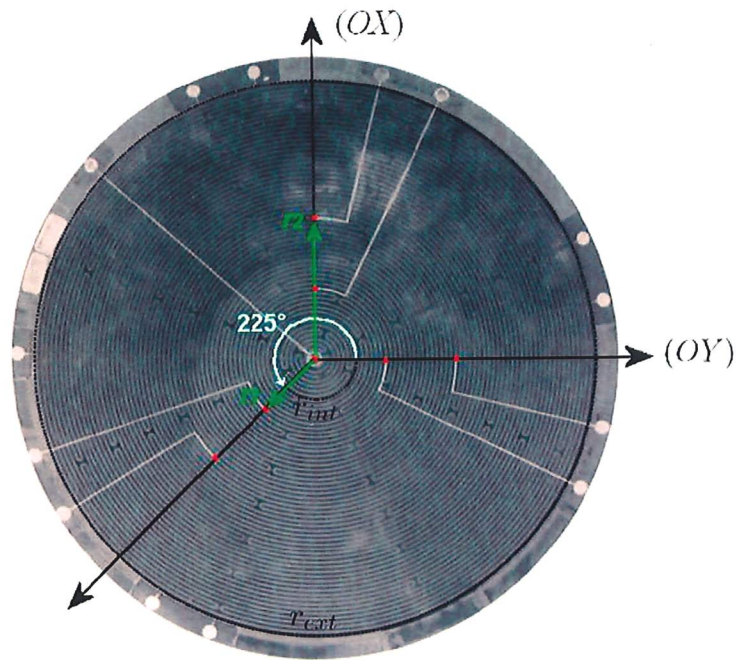


Figure 2: Upper face of the heater.

An IR pyrometer focused on the centre of the upper face of one sample, it ensures the measurement of the mean transverse thermal gradient. The vacuum chamber is equipped with a ZnS window through which pyrometer measurements are performed. At last, thin rubber sheets are placed between the composite samples and the heater to limit the roughness effect, and thus to ensure a good interface thermal contact, the total thickness is 0.6 mm.

Two thermal-regulated plates are located on both sides of the assembly. They ensure the temperature control of the assembly by radiation. Moreover, in order to prevent lateral heat losses, a barrel heater band is placed around the vacuum chamber to ensure the vacuum chamber wall temperature. These elements can be observed in Figures 3a and 3b.

To be tested by this device, two identical samples of the same material are required. Their shape is circular, with a radius equal to the heater one. The maximum thickness is 50mm in the actual design. Both samples have to be oriented along the same direction when they sandwich the heater.

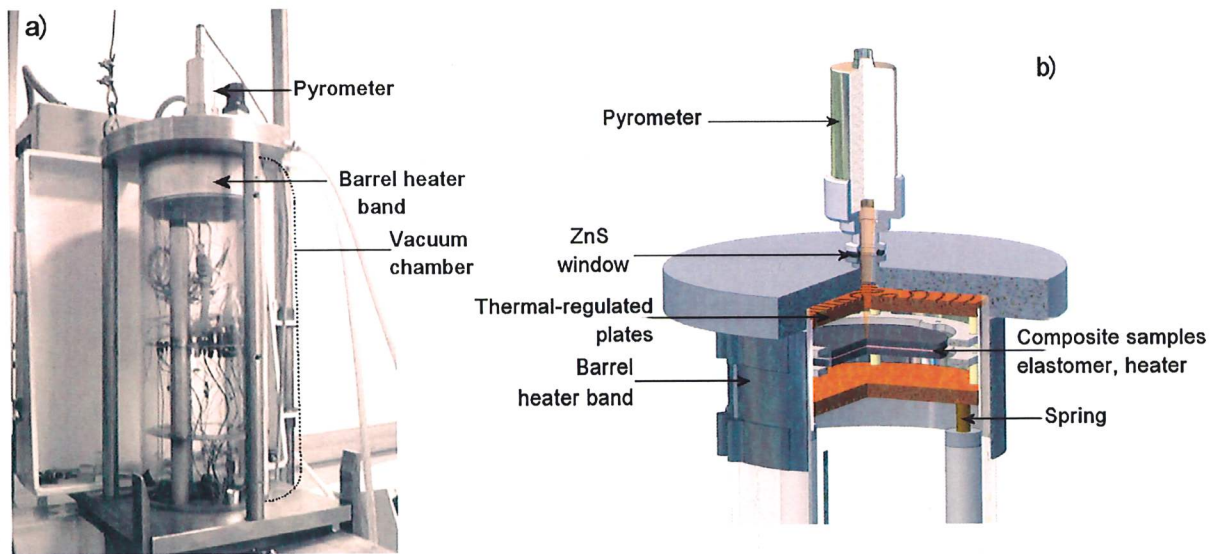


Figure 3 (a) Main elements of the experimental device. (b) Zoom on the system assembly.

Figure 3b sketches some elements of the measurement devices. One can observe in this figure, the tightening system of heater between the composite samples. The tightening system is composed of insulating rings that compress the samples on the heater (and elastomer sheets). All the system is developed on springs adaptable to sample thickness. Note that for any sample thickness, the upper face of the upper composite sample always remains at the same distance from the pyrometer and thus at the focal distance.

The acquisition system employed is a Multiplexor HP 985A. It is linked to a computer and the acquisition is controlled with Bench Link Data Logger software. This acquisition system allows direct measurements of temperature. Nevertheless, the internal compensation system of the device provides a rough precision, because the system uses a unique local temperature for correcting the whole cold junctions. Thus, if the cold junction temperatures are not homogeneous, then some temperature bias appears. To prevent these effects, we used our own and unique cold junction reference, the temperature of which is perfectly controlled. It consists in making junctions, between the thermocouple wires and extension copper wires, in a massive aluminium block. This block is located in an insulated box under vacuum. Its own temperature is measured by a platinum probe (Pt 100) and used as reference temperature. The acquisition system is then, only used for voltage measurements.

Experimental protocol

The experiment consists in these successive steps:

1. Perform the assembly of the samples and heater thanks to a tightening system.
2. Locate this assembly in the vacuum chamber and connect thermocouples and power wires of the heater to the acquisition system.
3. Create a vacuum inside the chamber and set the temperature of thermo-regulated plates and of the barrel heater band to the measurement temperature. Once all the thermocouples of the heater and the pyrometer indicate the isothermal state of the assembly, the experiment can start.
4. At $t = 0$ the heater (internal part or both parts) is powered. Heat flux is dissipated through the samples, and temperature rises are recorded by the thermocouples and the pyrometer.
5. At $t = t_{\text{end}}$, the data acquisition is stopped. The data are stored into a result file.
6. This file is then used as input data for estimating the effective thermal properties of the composite samples, according to an inverse heat conduction method.

The aim of the developed identification process is to determine the effective thermal properties of an orthotropic structure. The set of unknown parameters to be determined, involves the specific heat and the components of the thermal conductivity tensor. The thermal conductivity tensor of an orthotropic material in the coordinate system of the main directions (Oxyz) is diagonal

$$\Lambda_{(Oxyz)}^c = \begin{bmatrix} \lambda_{xx}^c & 0 & 0 \\ 0 & \lambda_{yy}^c & 0 \\ 0 & 0 & \lambda_{zz}^c \end{bmatrix} \quad (1)$$

The main directions are supposed to be orthogonal. We naturally consider the transverse direction (Oz), which is the sample thick-direction, as one of the main direction.

Concerning the two other main directions, (Ox) is the direction along which the planar thermal conductivity is the most important, and thus (Oy) the orthogonal direction to the two first ones. Taking the example of a pure unidirectional CFRP (all the carbon fibres are oriented along the same direction), (Ox) then correspond to the fibre direction (since

the thermal conductivity along this direction is the most important); (Oz) is the transverse direction; and (Oy) is the planar direction orthogonal to the fibre direction. Except in some peculiar cases (e.g. unidirectional composites), composite thermal main directions are generally unknown.

Let us consider the coordinate system of the heater (OXYZ). In this coordinate system, the composite thermal conductivity tensor can be written as

$$\Lambda_{(OXYZ)}^c = \begin{bmatrix} \lambda_{XX}^c & \lambda_{XY}^c & 0 \\ \lambda_{XY}^c & \lambda_{YY}^c & 0 \\ 0 & 0 & \lambda_{ZZ}^c \end{bmatrix} \quad (2)$$

The objective of the method is to estimate simultaneously these five parameters as well as the specific heat. Then, knowing $\Lambda_{(OXYZ)}$, it is easy to find the main directions in which this tensor is diagonal [2] and the diagonal components of $\Lambda_{(Oxyz)}$. The rotation angle between coordinates (Oxyz) and (OXYZ) is named θ .

An inverse method is used for estimating these parameters. The direct heat conduction problem is solved using a 3-D finite element solver. Identification of the unknown composite thermal properties consists in minimizing a least square criterion based on the differences between the observations (measured temperatures) and the calculated temperatures (direct problem) at the same locations.

2.1 Spatial fields: Finite Element geometry

The assembly (composite sample / elastomer sheet / heater / elastomer sheet / composite sample) being symmetrical, the thermal problem is reduced to the geometry presented in Figure 4. The spatial domain of the model equations involves three sub-fields: Ω_1 for the heater, Ω_2 for the elastomer, and Ω_3 for the composite sample.

Subscripts 1,2 and 3 will be more generally used for notifying properties or variables of the heater, elastomer and sample, respectively.

Heater thickness being $e_1 = 0.5 \cdot 10^{-3}$ m, half-thickness is represented in the geometry.

The mid-plane ($OXYZ = 0$) of the heater is also a symmetry plane of the assembly. The

thickness of the rubber sheet, placed between the heater and the sample, is $e_2 = 0.1 \cdot 10^{-3}$ m, the composite sample thickness is named e_3 .

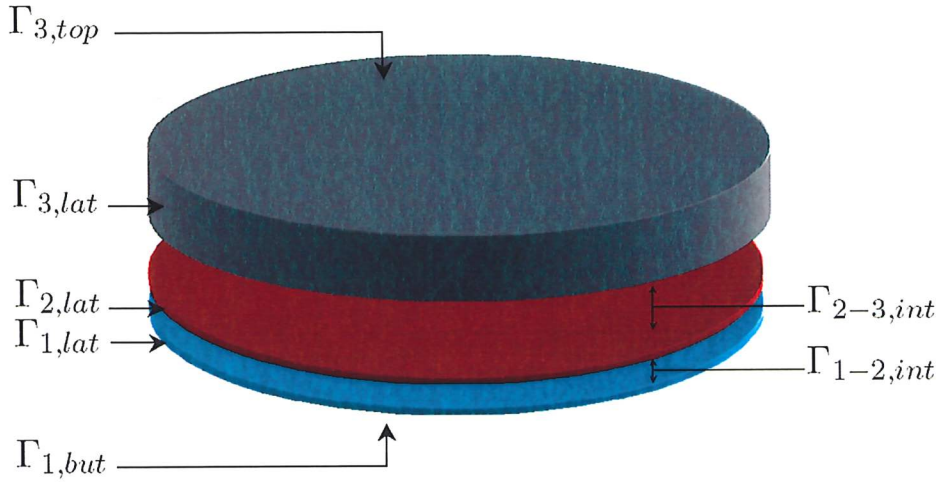


Figure 4: Finite Element geometry scheme containing heater, elastomer and composite fields.

2.2 Temperature fields

At the initial time of the experiment, heater is off, the temperatures of both composite samples and heater are uniform and equal to the vacuum chamber one, so $T(x, y, z, t=0) = T_\infty$ in Ω . For $t \in]0, t_f]$ a uniform heat flux is dissipated by the heater. This heat flux is modelled with a heat flux density $\phi(x, y)$ applied on the mid-plane: $\Gamma_{1,but}$. $\phi(x, y)$ is experimentally calculated from the measurement of the power delivered to the heater and from the heater electrical resistance.

The lateral faces $\Gamma_{1,lat}$, $\Gamma_{2,lat}$, $\Gamma_{3,lat}$ and the upper face of the composite sample $\Gamma_{3,top}$ are submitted to radiative boundary conditions. The emissivity of the external surface of the composite sample is denoted ε . Its influence will be later addressed.

Finally, the contacts between the layers heater-elastomer and elastomer-composite are not perfect, some temperature discontinuities can occur. They are modelled with thermal contact resistances, denoted $R_{tc_{1-2}}$ and $R_{tc_{2-3}}$ but we assumed they are equal and denoted R_{tc} . This hypothesis seems at first sight to be strong since it depends, for example, on the surface roughness of the composite. However, it was difficult to estimate two distinct parameters. Its influence will be later addressed too.

Then, the temperature fields $T_i(x, y, z, t)$, $i = 1, 2, 3$, are obtained by solving the following set of equations

$$\rho_i C p_i \frac{\partial T_i}{\partial t} = \nabla \cdot (\Lambda_i \nabla T_i), \text{ on } \Omega_i, 0 < t < t_f \quad (3)$$

$$n \cdot (\Lambda_i \nabla T_i) = \phi(x, y), \text{ on } \Gamma_{1,\text{but}}, 0 < t < t_f \quad (4)$$

$$n \cdot (\Lambda_i \nabla T_i) = \varepsilon \sigma (T_\infty^4 - T_i^4), \text{ on } \Gamma_{i,\text{lat}} \cup \Gamma_{3,\text{top}}, 0 < t < t_f \quad (5)$$

$$-\lambda_{1,zz} n_{1,z} \frac{\partial T_1}{\partial z} \Big|_{z=e_1} = \frac{T_1(z=e_1) - T_2(z=e_1)}{Rtc}, \Gamma_{1-2,\text{int}}, 0 < t < t_f \quad (6)$$

$$-\lambda_{2,zz} n_{2,z} \frac{\partial T_1}{\partial z} \Big|_{z=e_2} = \frac{T_2(z=e_2) - T_3(z=e_2)}{Rtc}, \Gamma_{2-3,\text{int}}, 0 < t < t_f \quad (7)$$

with n , the unitary normal vector to the surface, ε the emissivity of the external surfaces, and Rtc the thermal contact resistance introduced to account for the non-perfect contacts: heater-elastomer and elastomer-sample. Note that Rtc is assumed to be spatially uniform.

The heater design offers two distinct heating configurations. Configuration A consists in powering the central part of the heater, whereas for configuration B, both central part and peripheral corona are powered to dissipate a known uniform heat flux on the entire sample faces that are in contact. Characteristic function of the dissipated flux $\chi_{\text{heater}}(x, y, z=0)$ is

$$\begin{aligned} \text{Configuration A: } \chi_{\text{heater}} &= 0, r_{\text{int}} < r < r_{\text{ext}} \\ &1, 0 < r < r_{\text{int}} \end{aligned} \quad (8)$$

$$\text{Configuration B: } \chi_{\text{heater}} = 1, 0 < r < r_{\text{ext}} \quad (9)$$

And the heat source is defined by

$$\phi(x, y, z=0, t) = Q(t) \cdot \chi_{\text{heater}}(x, y, z=0) \quad (10)$$

$Q(t)$ is a heat flux step

$$\begin{aligned} Q(t) &= 0, 0 < t < t_0 \\ &Q_0, t_0 \leq t < t_{\text{end}} \end{aligned} \quad (11)$$

where Q_0 is a spatially uniform flux density. Heating tracks of the heater have been specially designed for this purpose. The homogeneity of the heat flux has been experimentally confirmed using IR images and the micro-thermocouple histories [31]. Q_0 is set up by the experimenter. The duration t_{end} is defined so as to avoid too large temperature raises in the sample.

2.3 Sensitivity fields

Computation of the temperature sensitivity fields to each unknown parameters is of prime interest. On the one hand, sensitivities inform on the feasibility of the identification process, and permit to choose the optimal time window to get the measurement data. On the other hand, they directly play a role in the iterative estimation process.

The temperature sensitivity field to each component of the parameter vector $\beta = [\beta_j]$ in the sub-field Ω_i is defined by

$$X_{ij}(x, y, z, t; \beta) = \frac{\partial T_i(x, y, z, t)}{\partial \beta_j}, \quad j = 1 : m ; i = 1, 3 \quad (12)$$

In practice, all badly known constant data of the model equations could be treated as parameters for estimation. However, increasing the number of parameters to be estimated reduces the accuracy of the estimation process, and vice versa. In practice, the information relative to geometry like the sample thickness, the sample radius, and the thermocouple locations or others like the power dissipated in the heater can be measured with high accuracy, so there is no need for their estimation. At the opposite, the thermal conductivity tensor, the specific heat, the thermal contact resistance between the heater and the samples have to be determined. The unknown parameter vector is

$$\beta = [\lambda_{3XX} \quad \lambda_{3YY} \quad \lambda_{3ZZ} \quad \lambda_{3XY} \quad Cp_3 \quad Rtc] \quad (13)$$

The thermal properties of the heater and the elastomer are also obtained experimentally (see section 5).

Temperature sensitivity fields are thus obtained by differentiating the model equations (equations 3-7) with respect to each component of this parameter vector. For example, the following set of equations defines the sensitivity field of the component $\beta_1 = \lambda_{3XX}$

$$\rho_i C p_i \frac{\partial X_i(\lambda_{3XX})}{\partial t} = \nabla \cdot (\Lambda_i \nabla X_i(\lambda_{3XX})) + \delta_{i,3} \frac{\partial^2 T_3}{\partial X^2}, \text{ on } \Omega_i \quad (14)$$

$$n \cdot (\Lambda_i \nabla X_i(\lambda_{3XX})) = 0, \text{ on } \Gamma_{1,\text{but}}, \quad (15)$$

$$n \cdot (\Lambda_i \nabla X_i(\lambda_{3XX})) = -4\varepsilon\sigma T_i^3 X_i(\lambda_{3XX}) - \delta_{i,3} \frac{\partial T_3}{\partial X}, \text{ on } \Gamma_{i,\text{lat}} \cup \Gamma_{3,\text{top}}, \quad (16)$$

$$-\lambda_{1,zz} n_{1,z} \frac{\partial X_1(\lambda_{3XX})}{\partial z} \Big|_{z=e_1} = \frac{X_1(\lambda_{3XX}, z=e_1) - X_2(\lambda_{3XX}, z=e_1)}{Rtc}, \Gamma_{1-2,\text{int}} \quad (17)$$

$$-\lambda_{2,zz} n_{2,z} \frac{\partial X_2(\lambda_{3XX})}{\partial z} \Big|_{z=e_2} = \frac{X_2(\lambda_{3XX}, z=e_2) - X_3(\lambda_{3XX}, z=e_2)}{Rtc}, \Gamma_{2-3,\text{int}} \quad (18)$$

with $\delta_{i,j}$ the Kronecker symbol. The sensitivity equations for the other parameters are obtained in a similar way.

It is observed that the sensitivity equations are similar to the heat equation, but they involve additional terms, coupled to the heat conduction model equations. Thus, like the temperature fields $T_i(x, y, z, t)$, the sensitivity fields are calculated with finite elements. To avoid storing the coupled terms, it is judicious to calculate simultaneously the whole fields T_i, X_{ij} ($j=1:m$) by solving a global set of equations, on the same mesh.

3 Optimal heater design

A special care has been brought to the design of the heater. The specification was to define a heater, as thin as possible, that allows to dissipate a spatially uniform heat flux as well as to measure temperatures. The choice led to a multi layer element on which are coated copper and constantan deposits. To design the heater power, the dimension of the heating parts, and the thermocouple location, numerical tests have been required and are described in the following sub-sections.

3.1 Dissipated heat flux

The first variable to set is the heat flux value to be dissipated through the samples and we set the following requirements to determine it. First, the value should not be too high to prevent an important temperature raise within the samples. In fact, the parameters to be estimated are supposed to remain constant within a low temperature range, from the initial isothermal state of the samples before the experiment starts. Thus, if the temperature raise is too important, it is not possible to assume that the experiment is performed within this temperature range. However, if the heat flux dissipated is too weak, then the measured temperature raises are also weak. The ratio "signal / noise" then decreases, and the estimation error increases.

Using the direct heat conduction model presented in the previous section, it is possible to predict the temperature increase of a composite versus the dissipated heat flux. Numerical tests led to consider that heat flux density values that go from $300\text{W}\cdot\text{m}^{-2}$ to $1300\text{W}\cdot\text{m}^{-2}$ are enough for estimating thermal properties of composite materials under study. Maximum temperature raises are then less than 10K. Note that, during the experiment, the heat flux value is a controlled variable.

3.2 Thermocouple locations

The influence of thermocouple locations on the estimated parameters is discussed by observing the spatial distribution of the temperature sensitivity fields to the parameters λ_{XX} , λ_{YY} , λ_{XY} , λ_{ZZ} and C_p . For example, they are plotted in Figure 5, at $t = 200\text{s}$. Sensitivity to C_p is large, at any time. Sensitivity to λ_{ZZ} is important only in the centre, and rapidly decreases to zero. On the contrary, although sensitivities to λ_{XX} and λ_{YY} are maximum in the centre, they exhibit a peak along (OX) and (OY) directions, respectively. A thermocouple must thus be located in the centre of the heater and two other should be along the (OX) and (OY) directions. Moreover, as the main directions are unknown, a third thermocouple has to be located in a third direction (different from (OX) and (OY)).

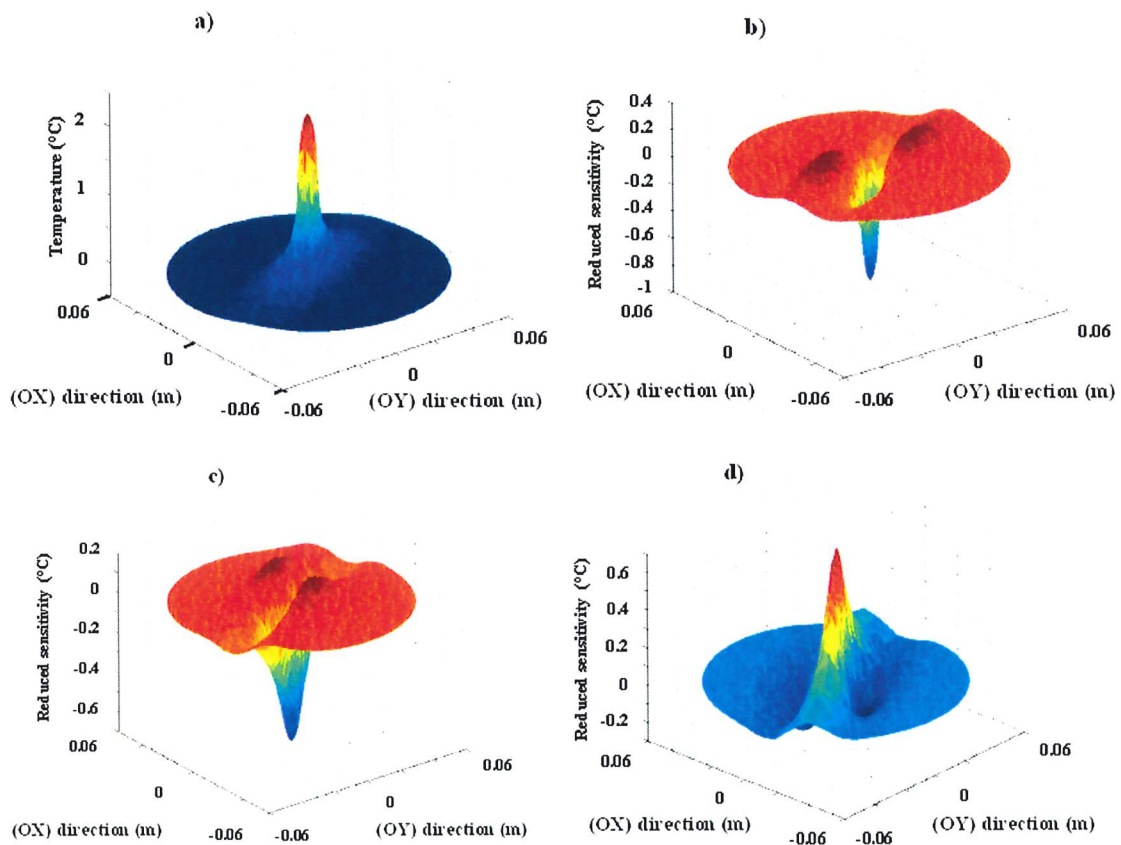
However, as usual in such optimal design process, the sensitivity fields depend on the parameter values to be estimated, and then the optimal sensor location implies some a

priori knowledge of these parameters. Thus, we consider a range of thermal conductivity values for composite materials that are standard for aeronautic structures: from $0.1 \text{ W.m}^{-1}.\text{K}^{-1}$ to $10 \text{ W.m}^{-1}.\text{K}^{-1}$. Different thermocouple locations were then studied; those for which sensitivities remain too weak or too much correlated were eliminated.

This study has led to place seven thermocouples in the heater plane (Figure 2)

- One on the heater center,
- three at a radius $r_1 = 10\text{mm}$,
- and three others at a radius $r_2 = 20\text{mm}$.

Placing thermocouples at two different radii permits to ensure they are sensitive to low thermal conductivities values as well as to greater ones.



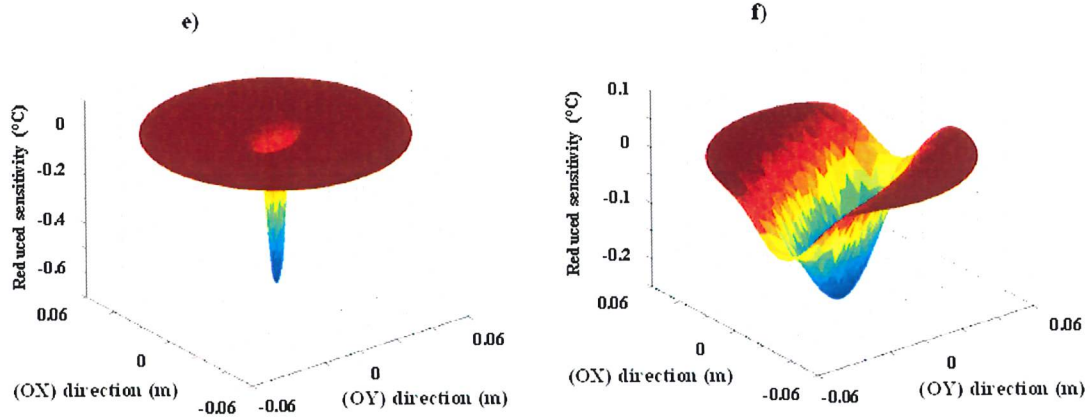


Figure 5: From left top to bottom right: temperature field (heater plane in configuration A), and temperature sensitivities to λ_{3XX} , λ_{3YY} , λ_{3XY} , λ_{3ZZ} and Cp_3 , computed at $t = 200s$.

4. Parameter estimations

4.1 Numerical experiment

In this section, the identification of the parameters by inverse method is addressed. The study of the feasibility and of the optimal estimation strategy requires the computation and the analysis of the temperature sensitivity fields to the estimated parameters. For this issue, we have simulated with the F.E. model presented previously, the thermal response of a standard fictive composite having the thermal properties given in table 1.

Property	Composite	Heater	Elastomer
λ_{xx} (W.m ⁻¹ .K ⁻¹)	5	0.7 ± 2%	0.24 ± 5%
λ_{yy} (W.m ⁻¹ .K ⁻¹)	0.7	0.7 ± 2%	Literature [32]: 0.15 – 0.31
λ_{zz} (W.m ⁻¹ .K ⁻¹)	0.6	1.0 ± 5%	
Cp (J.kg ⁻¹ .K ⁻¹)	1500	1500 ± 3%	1400 ± 5%
ρ (kg.m ⁻³)	1100	1500	1200

Table 1: Thermal properties of the composite, heater and elastomer considered for the test of parameter estimation.

The thermal properties of the heater has been determined experimentally from the experimental set-up, removing the domain associated to the composite sample in the F.E. model and using the developed inverse method detailed in the following subsection. The properties of the elastomer are given by the supplier. The applied heat flux density, Q , equals 1000W.m^{-2} and the R_{tc} value is assumed to be $10^{-4}\text{ m}^2.\text{K.W}^{-1}$.

4.2 Inverse method

The method we used to estimate the thermal properties of composite samples is based on the Ordinary Least Square (O.L.S.) estimation technique. Considering n_s the number of sensors and n_t the number of sampling times, the output model vector at the sensor locations can be defined by

$$Y(\beta)=[C].T(\beta), \text{ with } \dim(Y)=n_s \times n_t \quad (19)$$

where $T(\beta)$ is the finite element approximation of the solution of the model equations, and $[C]$ the sensor location matrix. Measurements, noted \tilde{Y} , are assumed to be corrupted only by an uncorrelated, zero mean, Gaussian, additive noise (σ_N = standard deviation). The estimation of $[\beta]$ consists in minimizing the O.L.S. criterion

$$S(\beta) = \|\tilde{Y} - Y(\beta)\|^2 \quad (20)$$

The model solution $Y(\beta)$ being non linear with respect to β , the minimum $\hat{\beta} = \text{argmin} S(\beta)$ is iteratively computed with the Gauss Newton algorithm. The iterative process is described in [33]-[34]. For each iteration k , the new estimate $\beta^{(k+1)}$ is computed by adding the parameter correction $d\beta^{(k)}$ to the estimate $\beta^{(k)}$ according to

$$d\beta^{(k)} = (X_s^{(k)t} . X_s^{(k)})^{-1} . X_s^{(k)t} (\tilde{Y}_s - Y_s(\beta^{(k)})) \quad (21)$$

The subscript "s" indicates that the variable is considered at the temperature sensor locations whereas the upperscript "t" denotes the transpose. The estimation of the parameters requires the difference between experimental temperature \tilde{Y}_s and the

computed model $Y_s(\beta^{(k)})$ and the temperature sensitivities to the parameter $X_s^{(k)}$. While the RMS (root mean square) between measured and predicted temperature is greater than the standard deviation of the measurement noise σ_N , the iterative process goes on. The values of the parameter vector are updated from equation 21, and serve as input parameter to the temperature F.E. solver. When the RMS become lower than σ_N , then the iterative process is stopped and the estimation error is evaluated.

The matrix $(X_s^{(k)t} . X_s^{(k)})$ has to be inverted for each iteration. Consequently, the parameters can be estimated only if the sensitivities computed at the measurement points remain linearly independent on the time interval considered. One way to investigate correlation is to simply plot the sensitivity coefficients versus each other. Because these plots can often be non-conclusive, it is recommended to compute the condition number of the matrix $(X_s^{(k)t} . X_s^{(k)})$

Estimation errors are evaluated from the standard following equation:

$$\text{re}(\beta_j) = \frac{\sigma_N}{\beta_j} \sqrt{\text{diag}_j(X_s^t X_s)^{-1}} \quad (24)$$

σ_N is the standard deviation of the measurement noise. It is evaluated during a short period prior to heating. *diag* indicates that only diagonal terms are considered.

4.2 Sensitivity study

The heater design offers two distinct heating configurations:

Configuration A

The configuration A consists in powering the only central part of the heater. For isotropic samples, the isotherm lines in the heater plane would be circular. However, for orthotropic composite materials, these isotherm lines are distorted in ellipses. X_1^* (λ_{3XX}), X_1^* (λ_{3YY}) and X_1^* (λ_{3XY}) are then different in the mid-plane.

Configuration B

In this configuration, both central part and peripheral corona are powered to dissipate a known uniform heat flux on the entire samples faces. In that case, the mid-plane (O, x,

$y, z = 0$) is (quasi-)isothermal, excepted close to the lateral boundary. Sensitivities to the parameters λ_{3XX} , λ_{3YY} and λ_{3XY} are then equal to zero.

The configuration A thereby permits to estimate all the parameters. Configuration B in contrast, is not sensitive to in-plane parameters that cannot be estimated using it. However, configuration B is not useless since both configurations may be used in a complementary way to estimate all the parameters with more accuracy. A strategy of identification may be then defined, but one must before detail the use of an inverse method for the estimation.

4.3 Validation of the inverse method / Estimation strategy

Optimal identification procedure can be analyzed from the sensitivity fields to the estimated parameters and from the property of the matrix $(X_s^{(k)t} . X_s^{(k)})$ built with the sensitivities at the sensor locations. This matrix depends on the heating configuration.

By normalizing this matrix in the form of the correlation matrix C_r [35], the relative error re on the final estimated parameters, due to the measurement errors, can be compared for both heating configurations A and B, and permit to explore different estimation strategies.

For example, we check the inverse method algorithm considering the thermal properties of a fictive composite material given in Table 1. Results were obtained with a standard deviation of noise σ_N equals to unity, 600 time points (time step $dt=0.25s$) and considering all the seven thermocouple locations.

Equations 25 and 26 give the final correlation matrices C_A, C_B obtained respectively for the heating configurations A and B

$$C_A = \begin{bmatrix} 1 & 0.3491 & 0.5421 & -0.9683 & 0.6336 & -0.7285 \\ \text{sym} & 1 & 0.4861 & -0.9674 & 0.6941 & -0.6492 \\ \text{sym} & \text{sym} & 1 & -0.4573 & 0.3114 & -0.9533 \\ \text{sym} & \text{sym} & \text{sym} & 1 & -0.5622 & 0.6464 \\ \text{sym} & \text{sym} & \text{sym} & \text{sym} & 1 & -0.3958 \\ \text{sym} & \text{sym} & \text{sym} & \text{sym} & \text{sym} & 1 \end{bmatrix} \quad (25)$$

$$C_B = \begin{bmatrix} 1 & 0.9292 & -0.9835 \\ \text{sym} & 1 & -0.8851 \\ \text{sym} & \text{sym} & 1 \end{bmatrix} \quad (26)$$

For C_A , the correlation parameters are given for λ_{3XX} , λ_{3YY} and λ_{3XY} , λ_{ZZ} , C_{pc} , and R_{tc} from the left to the right and from the top to the bottom of the matrix. For C_B , the correlation parameters are given for λ_{ZZ} , C_{pc} , and R_{tc} only. The relative errors associated to the estimated parameters when we carry out one experiment (i.e. heating configuration A or B) are presented in the Table 2.

Parameter	One experiment		Two experiments	
	Relative error	Relative error	Relative error	Configuration
	re _A (%)	re _B (%)	re (%)	
	Configuration	Configuration		
	A	B		
$\lambda_{3XX} (W.m^{-1}.K^{-1})$	1.01	-	0.13	A
$\lambda_{3YY} (W.m^{-1}.K^{-1})$	1.01	-	0.48	A
$\lambda_{3XY} (W.m^{-1}.K^{-1})$	1.29	-	0.70	A
$\lambda_{3ZZ} (W.m^{-1}.K^{-1})$	1.53	0.41	0.41	B
$C_{pc} (J.kg^{-1}.K^{-1})$	0.62	0.06	0.06	B
$R_{tc} (m^2.K.W^{-1})$	5.16	0.33	0.33	B

Table 2: Relative estimation error on thermal properties of the fictive composite material (see table 1) according to the employed strategy (one or two experiments).

In the light of these results, two strategies can be employed.

- The strategy “just A” permits to estimate all the six parameters with only one experiment. Nevertheless, we have noticed that the estimation errors decrease with configuration B for the last three parameters.
- Another strategy “B before A”, consists in performing two experiments, using both configurations: and in estimating three parameters at each experiment. With configuration B first, the parameters: λ_{ZZ} , C_{pc} , and R_{tc} are estimated more

accurately than with configuration A. It is important to notice that this estimation is possible because it is not dependent on the in-plane thermal conductivities, the sensitivities to λ_{3XX} , λ_{3YY} and λ_{3XY} , being equal to zero. Once the parameters λ_{ZZ} , C_{pc} , and R_{tc} have been estimated, the use of configuration A permits to estimate the three other parameters: λ_{XX} , λ_{YY} , and λ_{XY} . Thus, all the parameters are estimated in two steps. Conducting the estimation in two experiments, relative errors are lower (Table 2), meaning that the estimation is then more accurate.

The best strategy is therefore a balance between experiment duration and accuracy results. Although the second strategy provides more accurate estimations, it is obviously more time consuming than the first one since two experiments have to be realized, instead of one. Even if the heating time is rather rapid, the waiting time to be isothermal before starting the second experiment can be long (more than two hours).

5 Measurement of thermal properties of the heater

5.1 Heater thermal properties

The heater is one of the most important features of the proposed measurement device. This central probe constitutes both a heat source and temperature sensor. Its thermal properties have to be determined to perform the inverse process. The heater being composed by a stack of Kapton discs, on which copper conductive tracks and thermocouples are coated, the whole being taped with glue, measuring these properties is far from obvious. Moreover, this heterogeneous material has not isotropic properties. Looking at its structure, we assume that its thermal conductivity tensor has only two distinct components: a radial λ_r^h and a transverse one λ_{zz}^h . Thus the parameters to be estimated are

$$\Lambda_{(OXYZ)}^h = \begin{bmatrix} \lambda_r^h & 0 & 0 \\ 0 & \lambda_r^h & 0 \\ 0 & 0 & \lambda_{zz}^h \end{bmatrix} \quad (27)$$

We use the heating configuration A to estimate these thermal properties. The heater is placed in a vacuum chamber. No sample or elastomer sheet sandwiches it. The only central part of the heater is powered, and thermocouple responses are recorded. The inverse method led to the values given in Table 1, section 4.1.

5.2 Elastomer thermal properties

The silicon elastomer sheets used in the experiment are very thin (0.1 mm). A DSC (differential scanning calorimeter) was employed to estimate its specific heat. The thermal conductivity was given by the supplier. Results are compared to literature [32] data (see Table 1).

5.3 Emissivity of the black paint

The external surfaces of the tested composite samples are painted with a black paint: Velvet coating 811-21 from 3M® Corporation. The mean emissivity at the ambient temperature is 0.9.

6. Validation on PMMA material

In order to validate the proposed measurement method, tests on isotropic material with well-known thermal properties are realized. PMMA is an isotropic homogeneous material, whose thermal conductivity and specific heat have already been characterized. Two PMMA discs, 5mm thick, were instrumented with four thermocouples so has to measure the temperature rise inside the PMMA. This precaution allows to know if the F.E. model is able to predict accurately the temperature raise inside the tested samples. The locations of thermocouples (K-type, 80 μ m) placed in small grooves into PMMA samples, are indicated on Figure 7. External and lateral surfaces of the samples were recovered with a thin layer of black paint, whose emissivity was characterized: $\varepsilon = 0.9$.

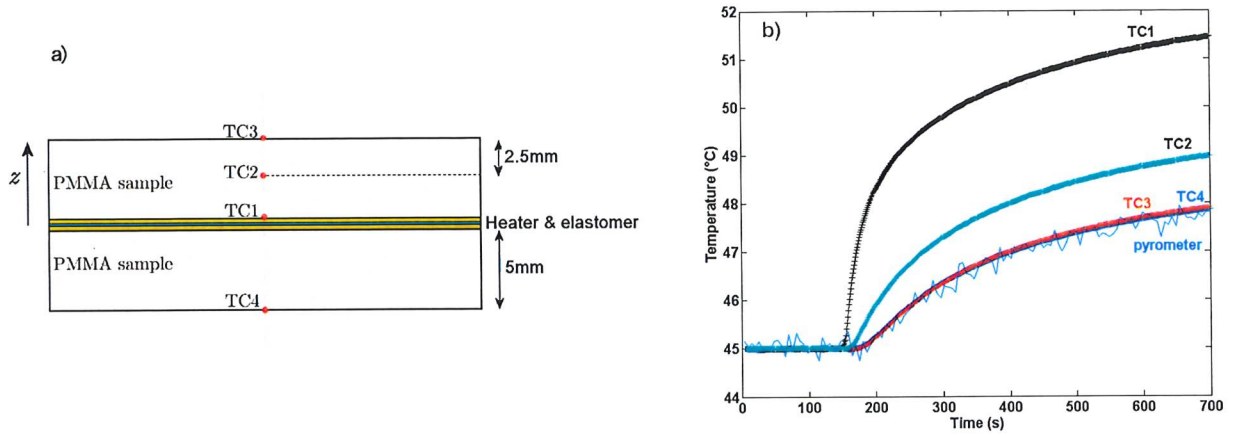


Figure 6: (a) Schematic illustration of the assembly. Four K-type thermocouples (TC1, TC2, TC3, TC4) are located into the PMMA sample. (b) Evolution of temperature measured by thermocouples located into PMMA samples. Heating configuration A. $\phi=1030\text{W/m}^2$.

6.1 Validation of symmetrical assumption

PMMA sample instrumentation permits to detect if the heat flux dissipated by the heater is well shared in two equal parts in both samples. We can observe in figure (Figure 7) that the temperature raises of the thermocouples located on the external faces (TC3 and TC4) of the PMMA samples, are nearly equal. These results obtained under configuration A (central heating only), validate the hypothesis of symmetrical assembly. Moreover, one can notice that the pyrometer results are in agreement with thermocouple ones. Similar results are obtained under heating configuration B.

6.2 Estimation of PMMA properties

PMMA material being isotropic, only three parameters have to be estimated. Then, the parameter vector to estimate is

$$\beta = [\lambda^{\text{PMMA}} \quad C_p^{\text{PMMA}} \quad R_{tc}] \quad (28)$$

Both configurations (A and B) can be used for estimating these parameters at 45°C. We first test configuration A, and then configuration B. Figure 8a shows the temperature evolution inside heater and PMMA samples when configuration A is employed. A

radial thermal gradient is observed. At the opposite, in Figure 8b, configuration B exhibits that heater thermocouples which provide nearly the same response. The heater plane is then isothermal. Estimated parameters are carried forward in the Table 3. Results are compared to literature data [36], and to pertinent measurements. These measurements were performed at 45°C on the PMMA material that was used for the experiments with a guarded hot plate (GHP) device for the thermal conductivity, and with a DSC for the specific heat.

Parameter	Configuration A (45°C)	Configuration B (45°C)	GHP / DSC (45°C)	Literature [36] (20°C)
λ^{PMMA} (W.m ⁻¹ .K ⁻¹) 1)	0.202 ± 2%	0.197 ± 0.5%	0.20 ± 2%	0.197
C_p^{PMMA} (J.kg ⁻¹ .K ⁻¹) 1)	1508 ± 1%	1491 ± 0.5%	1532 ± 2%	1380
Rtc (m ² .K.W ⁻¹)	4.10 ⁻³ ± 3%	3.10 ⁻³ ± 2%	-	-

Table 3: Estimated thermal properties at 45°C of PMMA using both heating configurations, and comparison with a dedicated guarded hot plate (GHP) and DSC measurements and data from literature [36].

Although a slight difference is observed between the results of both configurations, results are in agreement with pertinent measurements, and literature data. This validates the experimental measurement method in the case of an isotropic material.

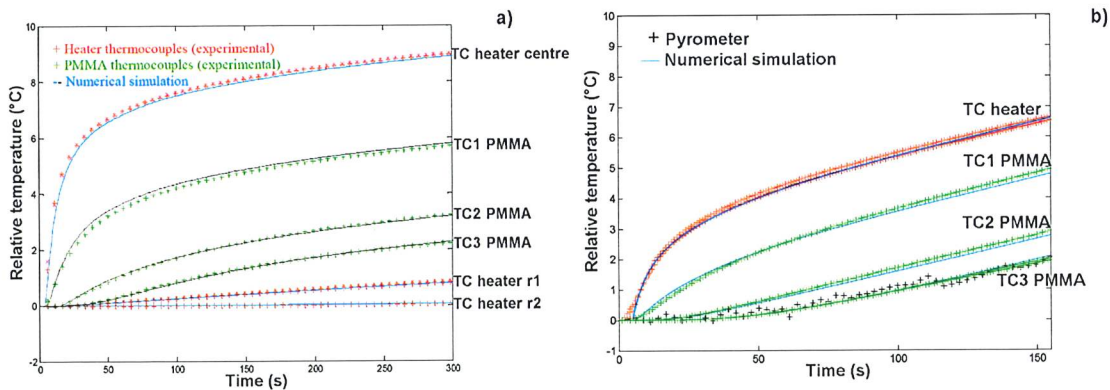


Figure 7: Experimental and numerical temperature rises. PMMA sample. (a) Configuration A. $\phi = 1030 \text{ W.m}^{-2}$. (b) Configuration B. $\phi = 435 \text{ W.m}^{-2}$.

7. Characterization of a unidirectional composite

We used the composite that was employed as reference material for the SFT Cross Bench [37] to validate the measurement method. As this composite is purely unidirectional, it is easy to detect the main longitudinal thermal conductivity (O_x) since it corresponds to the fibre direction. In order to know if the estimation of the orientation angle θ is accurate, in the following experiment the samples will sandwich the heater so that fibre direction makes an angle of 20° with the (O_x) direction of the heater. Experiments are realized at a measurement temperature of 45°C .

7.1 Heating configuration B

Using heating configuration B, the temperature raises illustrated in Figure 9 were obtained. One can notice that all the thermocouples provide nearly the same temperature responses. The measured temperatures lie between the average $\pm 0.1^\circ\text{C}$. Moreover, one can notice that a weak thermal gradient exists between the heater center and the peripheral corona. This may be due to the fact that the electrical resistances of the two heating tracks have not been perfectly balanced. The heat flux density dissipated by the central heating track is then lower than the one dissipated by the peripheral corona. Nevertheless, this problem was then solved by adjusting the values of the resistances used for the regulation.

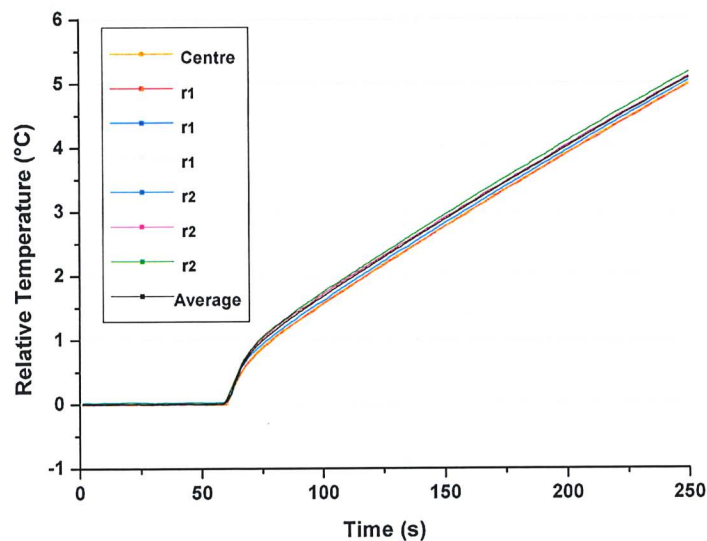


Figure 8: Experimental temperature rises measured by the heater thermocouples. Unidirectional composite sample. Configuration B. $\phi= 435\text{W/m}^2$.

From these results the inverse method was used so as to estimate the transverse thermal conductivity, the specific heat and the thermal contact resistance. Results are given in Table 4. Figure 10 shows that the temperature raise computed at the heater center is in agreement with the response measured by the two thermocouples located at the heater center. The same remark can be made for the temperature computed on the upper face of the composite sample, and the experimental temperature measured by the pyrometer.

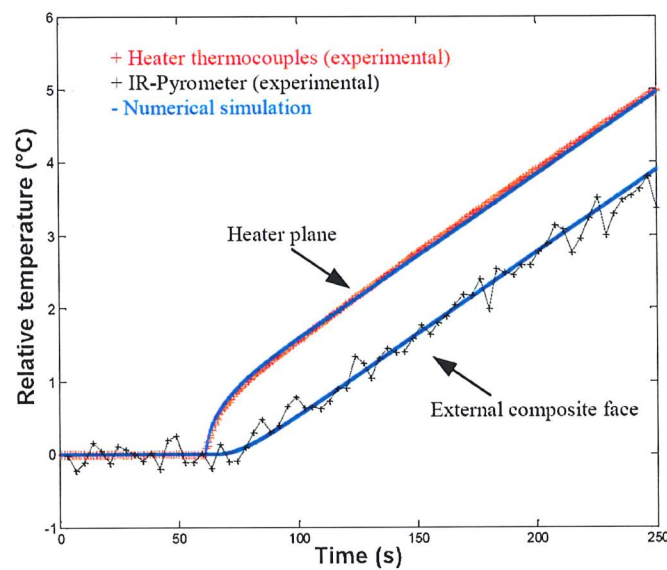


Figure 9: Experimental and numerical temperature rises. Unidirectional composite sample. Configuration B. $\phi= 435 \text{ W.m}^{-2}$.

7.2 Heating configuration A

The heating configuration A was then used to estimate λ_{3XX} , λ_{3YY} and λ_{3XY} . Figure 11 illustrates the agreement between experimental data and numerical computations once the inverse program has converged.

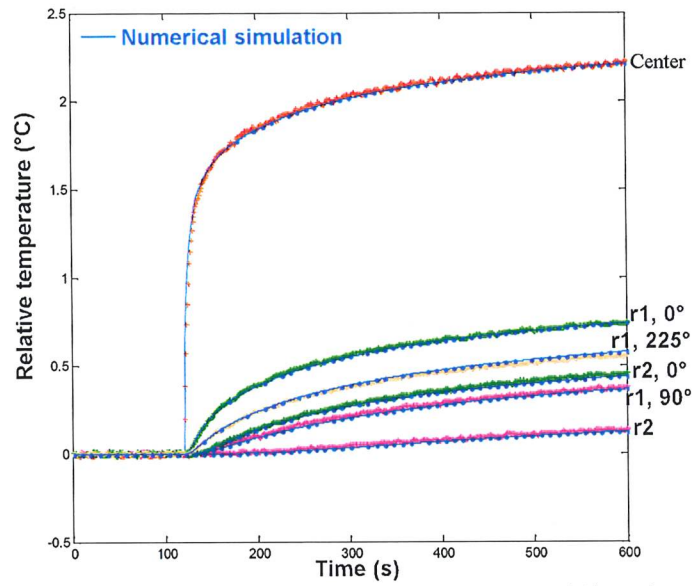


Figure 10: Experimental and numerical temperature rises. Unidirectional composite sample. Configuration A. $\phi = 1026 \text{ W.m}^{-2}$.

Results are given in the two following Tables 4 and 5. In the first one, thermal conductivity tensor is expressed in the heater coordinate system, whereas the latter is expressed in the composite main thermal direction coordinate system.

Parameters	Estimated value	Relative error (%) due to σ_N	Heating configuration
$\lambda_{3ZZ} (\text{W.m}^{-1}.\text{K}^{-1})$	0.62	2.23	B
$Cp_3 (\text{J.kg}^{-1}.\text{K}^{-1})$	1050	4.06	
$Rtc (\text{m}^2.\text{K}.\text{W}^{-1})$	5.10^{-4}	8.09	
$\lambda_{3XX} (\text{W.m}^{-1}.\text{K}^{-1})$	4.592	5.02	A
$\lambda_{3YY} (\text{W.m}^{-1}.\text{K}^{-1})$	1.368	1.09	
$\lambda_{3XY} (\text{W.m}^{-1}.\text{K}^{-1})$	-1.683	2.07	

Table 4: Estimated thermal properties at 45°C of a unidirectional composite using both heating configurations. The coordinate system is the one of the heater (O,X,Y,Z).

Parameters	Estimated value	GHP (40°C)	GHP (60°C)
$\lambda_{3xx} (\text{W.m}^{-1}.\text{K}^{-1})$	5.35	4.96	5.26
$\lambda_{3yy} (\text{W.m}^{-1}.\text{K}^{-1})$	0.662	-	-
$\lambda_{3zz} (\text{W.m}^{-1}.\text{K}^{-1})$	0.62	0.68	0.72

Cp_3 (J.kg ⁻¹ .K ⁻¹)	1050	992 (DSC)	1072 (DSC)
θ	23°	-	-

Table 5: Estimated thermal properties at 45°C of a unidirectional composite using the two heating configurations. Thermal conductivity tensor is given in the main thermal direction coordinate system (O,x,y,z).

The angle estimated between the two coordinate systems is $\theta = 23^\circ$. This result is close to the orientation we imposed for this experiment, which was 20° . The estimation of the main thermal directions of the composite is thereby efficient and is an other important specificity of the device since the orientation of the main directions is unknown in other measurement techniques. Note however, that this composite presents a strong thermal anisotropy ratio: $\lambda_{3xx}/\lambda_{3yy} = 8$. The results that we obtained with this method are in agreement with the others found for the Cross Bench [37] and with values obtained with other equipment in the laboratory (see Table 5). This is especially true for the specific heat and the longitudinal thermal conductivity λ_{3xx} . For λ_{3yy} and more especially for λ_{3zz} , it seems that the found values are in the lower part of the cloud of results. However, although these results are good, it remains difficult to provide additional conclusions, because the references we use to compare our results, is a cloud of scattered points. In some cases, the scattering is quite important (e.g. λ_{3yy} values go from 0.59 to 0.82 W.m⁻¹.K⁻¹ at 25°C). Finally, one can also notice that the thermal contact resistance estimated is low. This is due to the use of elastomer sheets that ensure a good thermal contact between the samples and the heater.

Conclusion

A new experimental device for the estimation of the thermal properties of composite materials has been developed. It was imagined to satisfy the main industrial requirements: reliability, accuracy, functionality, rapidity. It does not require sample instrumentation. The principle of the device is to dissipate a known heat flux through a thin heater sandwiched between two similar samples. It has been designed to ensure both thermal excitation and a measurement of temperature rises, which is the key-

element of the method. Its conception enables the heating of two distinct circular areas, which provides a choice in the strategy of parameter estimation. This heater, in which are located temperature micro-sensors allows the estimation of the whole thermal properties of composite samples, i.e. four components of the effective thermal conductivity tensor, the specific heat and, consequently, the thermal main directions in the plane. It is important to underline that few methods consider the question of the determination of the composite main directions.

A treatment of the data is performed to determine the thermal properties: the identification procedure is based on an inverse method and the direct problem is solved using a 3-D finite element solver. Temperature sensitivity fields, also computed with finite elements, have ensured the identification feasibility and were of prime interest to determine the optimal design of the heater such as the thermocouple locations and the power to be dissipated by the heater. They have also been useful to demonstrate the advantages and drawbacks of estimation strategies: the determination of the whole set of thermal parameters can be achieved with only one experiment but it is at the expense of the accuracy. At the opposite, two experiments are a better strategy if the accuracy is the driving criterion.

Tests on instrumented PPMA samples, for which the thermal properties are well-known, have been realized to validate the measurement technique. The results are close to those expected, which confirms the method. Consequently, the thermal properties of the unidirectional CFRP composite have been characterized. The results in the (Oyz) plan ($\lambda_{3yy}=0.662$ W/m.K and $\lambda_{3zz}=0.620$ W/m.K) given by the two-step strategy confirm the main directions and the weak anisotropy already predicted by the microstructure analysis [1].

New experiments are currently in progress to estimate thermal properties of composite materials at higher temperature level.

References

- [1] M. Thomas, N. Boyard, L. Perez, Y. Jarny, D. Delaunay. *Representative volume element of anisotropic unidirectional carbon – epoxy composite with high fibre volume fraction*. Composites Science and Technology. Vol 68. pp 3184-3192. 2008.
- [2] N. Ozisik. Heat conduction. John Wiley, Sons inc., 1993.
- [3] A. Degiovanni. *Conductivité et diffusivité thermique des solides*. Techniques de l'ingénieur, vol. R2 850, 1994.
- [4] Norme ISO 8302:1991. *Isolation thermique - détermination de la résistance thermique et des propriétés connexes en régime stationnaire -méthode de la plaque chaude gardée*. 1991.
- [5] Norme ISO 8894-1. *Matériaux réfractaires - Détermination de la conductivité thermique*. 1987.
- [6] H. Lobo. "Thermal conductivity and diffusivity" in "handbook of plastics analysis" ch. 5. Marcel Dekker, 2003.
- [7] Standard ISO 22007-1. *Plastics - Determination of thermal conductivity and diffusivity*. 2006.
- [8] Y. Jarny & P. Guillemet. *Estimation simultanée de la conductivité thermique et de la chaleur spécifique de matériaux orthotropes*. pages 609–614, Congrès SFT, 2001.
- [9] S.E. Gustafsson. *Transient plane source techniques for thermal conductivity and thermal diffusivity measurements of solid materials*. Rev.Sci. Instrum., vol. 62(3), pages 797-804, 1991.
- [10] M. Gustafsson, E. Karawacki & S.E. Gustafsson. *Thermal conductivity, thermal diffusivity and specific heat of thin samples from transient measurement with Hot Disk sensors*. Rev. Sci. Instrum.,vol. 65(12), pages 3856-3859, 1994.
- [11] C. Gobbé, S. Iserna & B. Ladevie. *Hot strip method: application to thermal characterisation of orthotropic media*. International Journal of Thermal Sciences, vol. 43, pages 951–958, 2004.
- [12] A.B. Donaldson & R.R.E. Taylor. *Thermal diffusivity measurement by a radial heat flow method*. J. Appl. Phys., vol. 46, pages 4584–4589,1975.
- [13] A. Degiovanni & M. Laurent. *Une nouvelle méthode d'identification de la diffusivité thermique par la méthode flash*. Rev Phys Appl, pages 229–237, 1986.

- [14] A. Degiovanni, J.C. Bastale & D. Maillet. *Mesure de la diffusivité longitudinale de matériaux anisotropes*. Rev Gén Therm, vol. 35, pages 141–147, 1996.
- [15] D. Demange, P. Beauchike, M. Bejet & R. Casulleras. *Mesure simultanée de la diffusivité thermique selon les deux directions principales d'un matériau*. Rev C and I Therm, vol. 36, pages 755–770, 1997.
- [16] M. Lachi & A. Degiovanni. *Détermination des diffusivités thermiques des matériaux anisotropes par méthode flash bidirectionnelle*. J. Physique III, vol. France 1, pages 2027–2046, 1991.
- [17] J.C. Krapez, L. Spagnolo, M. Frie, H.P. Maier & G. Neuer. *Measurement of in-plane diffusivity in non-homogeneous slabs by applying flash thermography*. Int. J. Therm. Sc., vol. 43, pages 967–977, 2004.
- [18] L. Spagnolo, J.C. Krapez, M. Frie, H.P. Maier & G. Neuer. *Flash thermography with a periodic mask : profile evaluation of the principal diffusivities for the control of composite materials*. SPIE Conference: Thermosense XXV, Orlando (USA), April 21-25 2003.
- [19] B. Rémy, A. Degiovanni & D. Maillet. *Measurement of the In-plane Thermal Diffusivity of Materials by Infrared Thermography*. International Journal of Thermophysics, vol. 26(2), pages 493–505, 2005.
- [20] I. Philippi, J.C. Batsale, D. Maillet & A. Degiovanni. *Measurement of thermal diffusivities through processing of infrared images*. Rev.Sci. Instrum., vol. 66(1), pages 182–191, 1995.
- [21] B. Hay, J-R. Filtz, J. Hameur & L. Rongione. *Uncertainty of thermal diffusivity measurements by laser flash method*. Cinquième conférence des propriétés thermophysique, Colorado, USA, 2003.
- [22] R.C. Heckman. *Finite Pulse-time and Heat-loss Effects in Pulse Thermal Diffusivity Measurements*. TJ. Appl. Physics, vol. 44(4), pages 1455–1460, 1973.
- [23] J.A. Cape & G.W. Lehman. *Temperature and Finite Pulse-Time Effects in the Flash Method for Measuring Thermal Diffusivity*. J. Appl. Physics, vol. 34, page 1909, 1961.
- [24] J.A. McKay & J.T. Schriempf. *Corrections for Non-uniform Surface Heating Errors in Flash Method Thermal Diffusivity Measurements*. J.Appl. Phys., vol. 47(4), pages 1668–1671, 1976.

- [25] A.J. Angstrom. *Annalen der Physik und Chemie* 114, 33, (1861) ; (also in *English translation*). *Phil. Magazine and J. of Science*, vol. 25, page 130, 1863.
- [26] L. Autrique, J.J. Serra & E. Scheer. *Microscale thermal characterization by inverse method in the frequency domain*. World Congress IFAC, Pragues, Czech Republic, July 2005.
- [27] A. Griesinger, W. Heidemarm & E. Halme. *Investigation on measurement accuracy of the periodic hot-wire method by means of numerical temperature field calculations*. *Int. Comm. Heat Mass Transfer*, vol. 26(4), pages 451–465, 1999.
- [28] J.J. Serra & L. Autrique. *Microscale thermal characterization of reinforced composites by photothermal microscopy data inversion*. 5th international conference on inverse problems in engineering: Theory and Practice, vol. Cambridge, England, 2005.
- [29] D. Rochais, H. Houëdec, F. Enguehard, J. Jumel & F. Lepoutre. *Microscale thermal characterization at temperatures up to 1000_C by photoreflectance microscopy. Application to the characterization of carbonfibres*. *J. Phys. D: Appl. Phys.*, vol. 38, pages 1498–1503, 2005.
- [30] C. Pradere, J.M. Goyheneche, J.C. Batsale, S. Dilhaire & R. Pailier. *Thermal diffusivity measurements on a single fiber with microscale diameter at very high temperature*. *International Journal of Thermal Sciences*, vol. 45, pages 443–451, 1995.
- [31] M. Thomas. *Propriétés thermiques de matériaux composites : caractérisation expérimentale et approche microstructurale*. PhD thesis. Université de Nantes. 2008.
- [32] D. Hands. *The thermal transport properties of polymers*. *Rubber Chemistry and Technology*, 1977, vol. 50, pages 480–522, 1977.
- [33] K. Levemberg. *A Method for the solution of certain problems in least squares*. *Quart. Appl. Math.*, vol. 2, pages 164–168, 1944.
- [34] J.V. Beck & K.J. Marnoldorlet. *Parameter estimation of non-linear parameters*. John Wiley & Sons New York, 1977, vol. 2, pages 164–168, 1977.
- [35] R.E. Van Walpole & R.H. Myers. *Probability and statistics for engineers and scientists*. 5th Ed., Macmillan Publishing Co., NY, USA, 1993.
- [36] D.W. Van Krevelen. *Properties of polymers*. Elsevier, Amsterdam, 1990.

- [37] Y. Jarny, Y. Murer. Round robin test « Thermal modelling and characterization of monolithic composite materials”. Journées de la société Française de Thermique. 18-19 may 2005. Toulouse, France (Active link at the end of the following web page <http://www.polytech.univ-nantes.fr/ltn/conducomp.dwt>).